STUDY OF ZIRCONIUM BASED ALLOYS BY NEUTRON DIFFRACTION

M. Krůželová, S. Vratislav, M. Dlouhá

Department of Solid State Engineering, FNSPE, CTU, Trojanova 13, 120 00, Prague 2, Czech Republic
monika.kruzelova@fjfi.cvut.cz

Keywords:

diffraction, texture analysis, zirconium based alloys

Abstract

Neutron diffraction is a very powerful tool in texture analysis of zirconium based alloys used in nuclear technique. In our work, the textures of two rolled sheets and three tubes were investigated by direct pole figures and inversion pole figures. The experiments were performed on the KSN-2 neutron diffractometer located at the research reactor LVR-15 in the Nuclear Research Institute, plc. Rez, Czech Republic. Texture development in zirconium and procedures for obtaining texture parameters (direct and inverse pole figures) are also described. Collected data were processed by software packages HEXAL and GSAS. It was found that the addition of alloying elements breaks the central area of basal pole figures of tube samples into two maxima. A characteristic split of the basal pole maxima tilted by 45° from the tangential direction toward the radial direction can be observed in basal pole figures of tubes. The (100) and (110) planes of tubes are oriented perpendicular to tube axis. Sheet samples prefer orientation of planes (100) and (110) perpendicular to rolling direction and orientation of planes (002) perpendicular to normal direction. The obtained results are characteristic for zirconium based alloys.

1. Introduction

The textured material usually exhibits anisotropic mechanical, physical and chemical properties. Preferred orientation occurs in both powder samples (shape texture) and compact samples (caused by mechanical or heat treatment of material) [1].

Looking on diffraction methods to measure textures mainly three different radiations are in use. These are X-rays produced by conventional X-ray tube or synchrotron, electrons and thermal neutrons. Basic differences of these radiations are based on interaction of the radiation with matter [2].

The main advantages of neutron diffraction arise from the high penetration of neutrons. The investigated sample volume is 10^4–10^6 higher than in the case of X-rays. Therefore, neutron diffraction presents an efficient tool for global texture investigations. The second advantage is easy sample preparation; surface preparation is not necessary [3].

This article deals with the use of neutron diffraction in texture analysis of zirconium based alloys. Zirconium has very low absorption cross-section of thermal neutrons, high hardness, ductility and corrosion resistance. Therefore, zirconium alloys are used in the nuclear industry (Zircaloy) as fuel rod cladding, especially in water reactors [4].

The work gives also a listing of structural parameters and texture characteristics of zirconium alloys. Textures of five samples were investigated by directpole figures and inversion pole figures.

2. Texture development in zirconium

2.1 Crystallographic characteristics of zirconium

Zirconium is an element of IV.B subgroup of the periodic system. Under normal conditions zirconium has a hcp crystal structure with the lattice parameters a = 0.3231 nmand c = 0.5141 nm [5]. Space group of this metal is $P6_3/mmc$.

The important directions in zirconium are slip directions <110> and <113>. Tab. 1 shows the important planes in zirconium [6].

Table 1. Important planes in zirconium.

Plane type	Miller indices
Basal plane	{002}
Prismatic planes 1st type	{100}
Prismatic planes 2nd type	{110}
Pyramidal planes 1st type 1st order	{1-11}
Pyramidal planes 1st type 2nd order	{102}

2.2 Deformation textures in zirconium alloys

Most of the texture measurements are related to the basal pole distribution which plays an important role. Less known is the distribution of prism or pyramidal plane poles. These are strong indicators for degree of annealingand, moreover are important for quantitative determination of textures, for example, by analysis of the orientation distribution function (ODF) [6].

In all hcp metals the final orientation of basal plane (002) is parallel to the direction of elongation -deviations from this preferred orientation exhibit characteristic differences between the hcp structures. Therefore, the textures of the hcp structures are categorized into three groups, according to the axial c/a ratio [6]. For metals and alloys with below-normal c/a axial ratio (e.g. zirconium) the position of the basal poles is tilted by +/-20-60° from the normal direction towards the transversal direction [6].

Deformation textures in tubing

Reduction in cross-section R_A can be achieved by reduction in wall thickness R_W, by reduction in diameter R_D or by any combination of R_W and R_D. Three extremes of the different

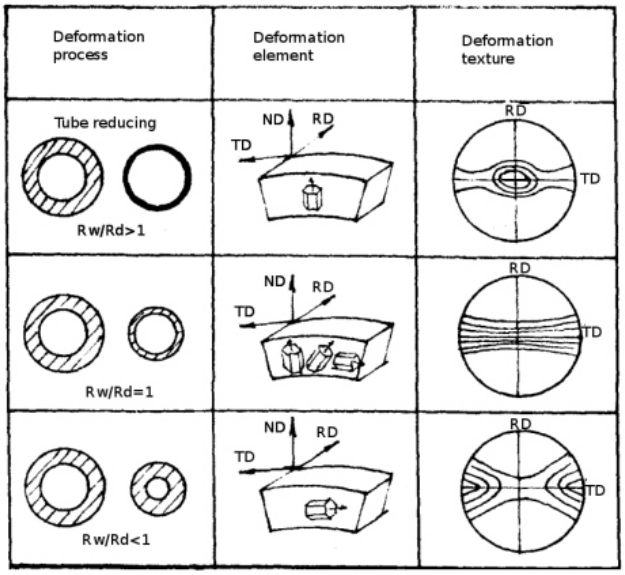

Figure 1. Expected basal pole figures for zirconium based alloys.

reduction ratios RW/ RD observed in zirconium alloys are discussed [6]:

- $R_W/ R_D > 1$ (Fig. 1a) – Tubes are mainly compressed in the radial direction, whereas the compressive forces in the tangential direction are comparatively small. A characteristic split of the basal pole maxima of +/-20 –40° tilted from the radial towards the tangential direction can be observed.
- $R_W/ R_D \sim 1$(Fig. 1b) – The deforming and compressive forces operate with equal strength in the radial and tangential directions. The result is a fiber texture with a random distribution of basal poles in the radial-tangential plane.
- If $R_W/ R_D < 1$ (Fig. 1c) – Tubes are mainly compressed in the tangential direction, whereas the compressive forces in the radial direction are comparatively small. A characteristic split of the basal pole maxima of+/-20 –40° tilted from the tangential towards the radial direction can be observed.

Deformation textures in sheet

During the rolling process, the sheet is compressed in the normal direction (ND), lengthened in the rolling direction (RD) and slightly changes dimension in the transverse direction (TD). The result is the texture which is identical to the texture in tubing for $R_W/R_D > 1$. This is to be expected since the stress-strain conditions are comparable [6].

Table 2. Chemical composition of material (rolled sheets).

Rolled Sheets	Element content [mass %]			
	Cu	Fe	Mo	W
Zrp	0.5	0.5	0.45	0.25

3. Experiment

The texture measurements of five zirconium samples were performed at diffractometer KSN-2 at Laboratory of Neutron Diffraction, Department of Solid State Engineering, Faculty of Nuclear Sciences and Physical Engineering using the TG-1 texture goniometer with automatic data collection[7]. The monochromatic neutrons having wavelength 0.1362 nm were used. The single-crystal Cu(200) was used asmonochromator. The KSN-2 diffraction device offers good intensity and the best resolution value of $d/d = 0.007$ in the region $d \sim 1.0 \div 0.1$ nm (d is interplanar spacing).

3.1 Samples

Rolled sheets

Sample Zrp was composed of 11 sheets of circular shape with a diameter of 50 mm. The thickness of one sheet was 0.25 mm. The sheets were cold –rolled with 92% reduction. Sample Zr1 was composed of 3 sheets of square shape, the side being 30 mm long. The thickness of one sheet was 1.1 mm. The sheets were cold –rolled with 50% reduction, annealed at 650 °Cand again cold-rolled with 50% reduction. Tab.2 shows the composition of sheet specimens.

Tubes

All tubes (Zry2, ZiT a ZrW) were extruded into an outside diameter of 50 mm and then cold-rolled with inter-annealing (700°C) to the final sizes. Tab. 3 shows the composition and parameters of tubes. There is tube length, $_e$ is outside tube diameter and $_i$ is internal tube diameter.

Table 3. Chemical composition of material (tubes).

Tubes	Element content							Tube parameters			R_w/R_D
	[mass %]			ppm							
	Sn	Fe	Cr	O	H	N	C	[mm]	[mm]	[mm]	
Zry2	1.46	0.21	0.09	1090	10	50	12	39.6	12.1	11.2	0.08
ZiT	1.39	0.25	0.11	1110	20	60	12	30	9.1	8	0.14
ZrW	1.42	0.26	0.12	1080	15	45	12	30	9.2	8	0.15

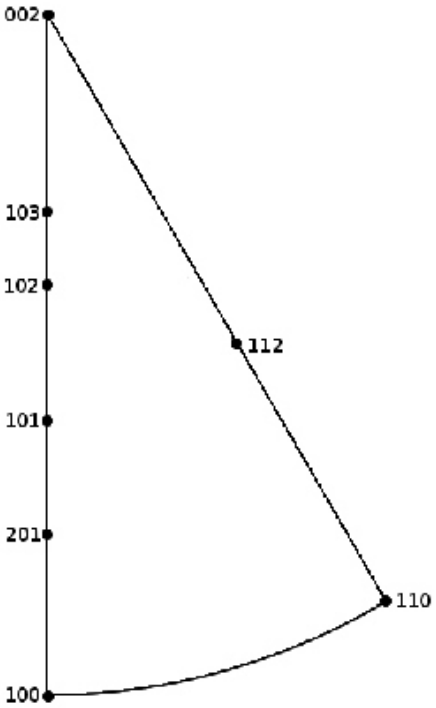

Figure 2. Distribution of poles in inverse pole figure.

3.2 Used methods

The result of texture measurements is represented by direct pole figures andinverse pole figures.

Direct pole figure

The direct pole figure is a stereographic projection of spatial distribution of poles of the particular plane to the project plane which is parallel to the significant sample plane. Direct pole figures were measured for (100), (002), (101), (110)and (102) reflections of samples Zr1, Zry2 and ZiT using the TG-1 texture goniometer. The step size was 5 °. The experimental data were measured in transmission or reflection arrangement. The measured data were corrected for absorption, irradiated volume and normalized using software package HEXAL [8].

Inverse pole figure

The inverse pole figure shows how the selected direction in the sample reference frame is distributed in the reference frame of the crystal.

In most cases, inverse pole figures are recalculated from the 3D ODF. However, inverse pole figures can also directly be measured by means of diffraction methods [8]. The sample is mounted in reflection geometry with its normal parallel to the direction of interest usually RD, TD, or ND and the reflected intensities are measured depending on Bragg angle.The resulting peak intensities are normalized to the intensities ofa standard sample with random texture (by using Mueller formula [8] and software package GSAS [9]).

The intensity ratios p_{hkl},q were calculated by Mueller formula[8] for (100), (002), (101), (102), (110), (103), (112) and (201) reflections for directions q = TD, ND, RD and direction between ND and TD (label as (0,45), see Tab. 4). Inverse pole figures were calculated for samples Zrp, Zry2, ZiT and ZrW.

Fig. 2 shows the distribution of poles in the inverse pole figure. Calculation procedure consisted of calculations of several poles given in the figure.

3.3 Results

Fig. 3 shows the obtained basal pole figures of samples ZiT, Zry2and Zr1 (using software package HEXAL). The calculated pole densities of selected hkl polesare show in Tab.4 (sample Zrp), Tab.5 (sample Zry2), Tab.6 (sample ZiT) and Tab.7 (sample ZrW).

Table 4. Calculated inverse pole figures of sample Zrp.

Miller indices	p_{hkl},TD	p_{hkl},ND	p_{hkl},RD
100	1.74	0.17	2.74
002	0.57	3.08	0.14
101	0.89	0.16	0.57
102	0.55	1.03	0.21
110	1.64	0.40	1.68
103	0.34	2.44	0.12
112	0.91	0.53	1.06

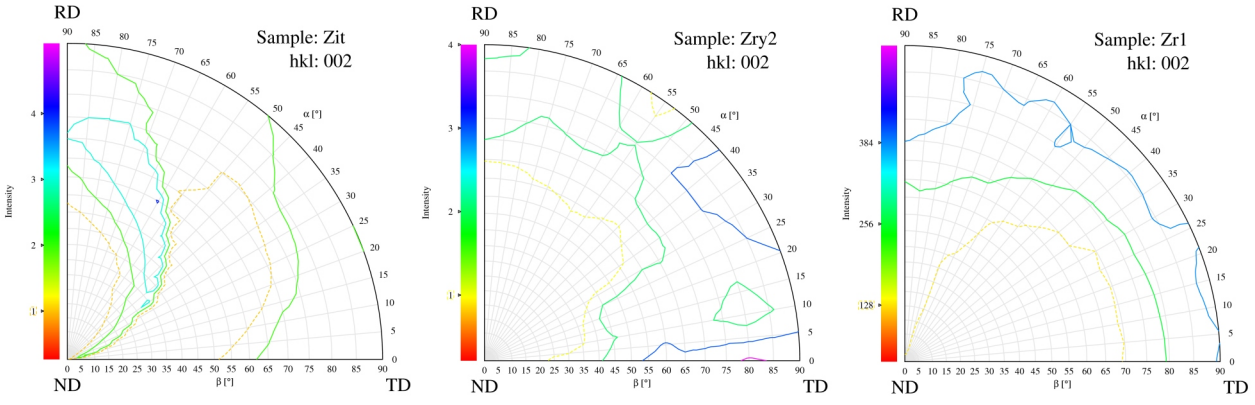

Figure 3. Comparison of basal pole figures of zirconium samples Zr1, Zry2, and Zit. System of coordinates is represented by ND, RD, and TD.

Table 5. Calculated inverse pole figures of sample Zry2.

Miller indices	p_{hkl}, TD	p_{hkl}, ND	p_{hkl}, RD	p_{hkl}, (0,45)	p_{hkl}, (45,45)	p_{hkl}, (90,45)
100	0.89	0.47	1.17	0.80	0.60	0.65
002	0.62	1.70	0.32	1.73	0.50	0.42
101	0.61	0.26	0.23	0.40	0.42	0.78
102	1.09	1.10	0.47	1.00	1.35	1.49
110	0.93	0.62	2.78	0.77	1.05	0.75
103	1.03	1.80	0.59	1.15	1.61	0.89
112	1.08	0.74	0.70	0.78	1.15	1.49

Table 6. Calculated inverse pole figures of sample ZiT.

Miller indices	p_{hkl}, TD	p_{hkl}, ND	p_{hkl}, RD	p_{hkl}, (0,45)	p_{hkl}, (45,45)	p_{hkl}, (90,45)
100	0.75	0.48	3.77	0.67	1.04	0.93
002	1.39	1.16	0.34	1.81	0.65	0.66
101	0.23	0.12	0.12	0.18	0.67	0.45
102	0.88	1.58	0.51	0.84	1.25	1.33
110	1.57	1.20	0.72	1.16	0.77	1.03
103	1.18	1.47	0.55	1.22	1.50	1.50

4. Discussion and Conclusions

The addition of alloying elements breaks the central area of basal pole figures of tube samples into two maxima – see Fig. 3 [10]. For (002) pole figure of Zr1, the position of the basal poles is tilted by 60° from the normal direction (ND) toward the transverse direction (TD). This is typical for metals and alloys with below-normal *c*/*a* ratio, e.g., zirconium, titanium and hafnium. A characteristic split of the basal pole maxima tilted from the tangential toward the radial direction for samples can be observed in basal pole figures for Zry2 and ZiT. Tubes were deformed by a high diameter and low wall thickness reduction ($R_W/R_D < 1$) [6]. Sample Zrp shows orientation of planes (002) perpendicular to normal direction ($p_{(002)}$, ND= 3.08, Tab. 4). It is not possible to determine (from the calculated pole densities of selected *hkl* of sample Zrp, Tab. 4) if the position of the basal poles is tilted by 60° from the normal direction (result observed from basal pole figure of sheet sample Zr1) because inverse pole figures were calculated only for several poles given in Tab. 6.

The (100) pole density maximumof Zrp sample is tilted from the rolling direction towards the transverse direction -planes (100) are oriented perpendicular to rolling direction. An analogous situation can be observed for planes (110).

Table 7. Calculated inverse pole figures of sample ZrW.

Miller indices	p_{hkl}, TD	p_{hkl}, ND	p_{hkl}, RD	p_{hkl}, (0,45)	p_{hkl}, (45,45)	p_{hkl}, (90,45)
100	0.44	0.65	2.95	0.47	1.35	0.06
002	1.85	1.17	0.40	2.40	0.47	0.51
101	0.14	0.23	0.14	0.02	0.68	0.60
102	0.75	0.66	0.50	0.66	1.40	1.43
110	1.17	1.67	0.79	1.30	0.56	0.46
103	1.65	1.13	0.54	1.14	1.53	1.49

The (100) planes of tubes are oriented perpendicular to tube axis. Angle position of (002) pole maximum of sample ZrW is tilted by 45° from the transverse direction toward the normal direction (Tab. 7). Similar situation occurs for samples Zry2and ZiT but the value of pole density is lower (Tab. 5 and Tab. 6). The pole densities presented for sample Zry2 (Tab. 5) differ from the pole densities for samples ZiT (Tab. 6) and ZrW (Tab. 7) because parameters of tubeswere significantly different.

Level of resulting texture and maxima position is different for the sheets and for the tubes. Substantial influence also has a final tube thickness. The results obtained are characteristic for zirconium based alloys (see [1], [11]).

References

1. H. Hsun, *Texture of metals*, Technical report, United States Steel Corporation Research Laboratory, 1974.
2. G. E. Bacon, *Neutron Diffraction*, 3rd ed., Oxford: Clarendon Press, 1975.
3. H. G. Brokmeier, *Advances and applications of neutron texture analysis*, Textures and microstructures, 33, 1999, pp. 13 – 33.
4. K. L. Murty, *Applications of Crystallographic Textures of Zirconium Alloys in the Nuclear industry*, Zirconium in the nuclear industry: Eighth International Symposium, ASTM STP 1023, L.F.P. Van Swam and C.M. Eucken, Eds. , American Society for testing and Materials, Philadelphia, 1989, pp. 570 – 595.
5. I. Kraus, *Struktura a vlastnosti krystalu*, Academia, Praha 2004.
6. E. Tenckhoff, *Review of Deformation Mechanism*, Journal of ASTM International JAI, 2, 2005.
7. M. Krůželová, *Studium vlastností slitin na bázi zirconia metodou neutronové difrakce*, Diplomová práce, ceské vysoké ucení technické v Praze, Fakulta jaderná a fyzikálne inženýrská, KIPL, 2010.
8. G.B. Harris. Philos Mag, 43, 1952, p. 113.
9. A.C. Larson, R.B. Von Dreele, *General Structure Analysis System (GSAS)*, Los Alamos National Laboratory Report LAUR 86-748, 1994.
10. Ch. S. Barrett, *Struktura kovu*, Nakladatelství ceskoslovenské akademie ved, 1959.
11. A. V. Nikulina, *Zirconium Alloys in Nuclear Power Engineering*, Metal Science and Heat Treatment, 46, 2004, pp. 458 – 462.